Title: Diverse biological processes coordinate the transcriptional response to nutritional changes in a *Drosophila melanogaster* multiparent population

Authors: Ng'oma E.[1,2], Williams-Simon P.A.[1], Rahman A.[1], King, E.G.[1]

[1] 401 Tucker Hall, University of Missouri, Columbia, MO 65211
[2] Corresponding Author

ORCIDs:
Ng'oma, E. https://orcid.org/0000-0002-6741-7922
Williams-Simon, P.A. https://orcid.org/0000-0003-1947-476X
King, E.G. https://orcid.org/0000-0002-9393-4720

Corresponding Author:

Enoch Ng'oma
Postdoctoral Scholar
401 Tucker Hall
University of Missouri
Columbia, MO 65211, USA

Email: ngomae@missouri.edu

Keywords: Coexpression; Differential Gene Expression, *Drosophila melanogaster;*

Abstract

Environmental variation in the amount of resources available to populations challenge individuals to optimize the allocation of those resources to key fitness functions. This coordination of resource allocation relative to resource availability is commonly attributed to key nutrient sensing pathways , mainly the insulin/TOR signaling pathway in laboratory model organisms. However, the genetic basis of diet-induced variation in gene expression is less clear. To describe the natural genetic variation underlying nutrient-dependent differences, we used an outbred panel derived from a multiparental population, the *Drosophila* Population Resource. We analyzed RNA sequence data from multiple female tissue samples, dissected from flies reared in three nutritional conditions: high sugar (HS), dietary restriction (DR), and control (C). A large proportion of genes in the experiment (19.6% or 2471 genes) were significantly differentially expressed for the effect of diet, 7.8% (978) for the effect of the interaction between diet and tissue type (LRT, adj. $P < 0.05$). Interestingly, we observed similar patterns of gene expression in DR and HS treated flies, response likely due to diet component ratios. Hierarchical clustering identified 21 robust gene modules showing intra-modularly similar patterns of expression across diets, all of which were highly significant for diet or the diet-tissue interaction effects (FDR adj.$P < 0.05$). Gene set enrichment analysis for different diet-tissue combinations revealed pathways and gene ontology (GO) terms (two-sample t-test, FDR q-value < 0.05). GO analysis on individual coexpressed modules likewise showed a large number of terms encompassing a large number of cellular and nuclear processes were observed (Fisher exact test, $P_{adj.} < 0.01$). Although a handful of genes in the IIS/TOR pathway including *Ilp5*, *Rheb*, and *Sirt2* showed significant elevation in expression, known key genes such as *InR*, *chico*, and other Ilps, and the nutrient-sensing pathways were not observed. Our results suggest that a broader network of pathways and gene networks mediate the diet response in our population. These results have important implications for future studies of diet responses in natural populations.

Background

Individuals can withstand changing nutritional conditions by flexibly adjusting the allocation of resources to competing life history traits, allowing populations to adapt and thrive. Individual ability to partition available nutrients and optimize fitness gains requires complex cooperation at multiple levels of functional and structural organization in tandem with prevailing conditions dictating nutrient availability. Changes in diet are associated with many phenotypic changes. For example, in many metazoan species, moderate nutrient limitation extends lifespan and delays age-related physiological decline [1–4]. In fluctuating resource conditions, this effect, in which the individual often shifts nutrients away from reproduction and towards somatic maintenance and repair may be adaptive, ensuring survival in bad conditions and reproduction when good conditions return [5, 6]. On the other hand, constant dietary excess such as diets high in sugar, promote obesity in many genetic backgrounds, accelerate the rate of aging, and reduce lifespan [7–10].

A large and growing body of literature points to endocrine pathways being involved in nutrient perception and balance in order to coordinate organismal response to diet change. Nutrient sensing mechanisms and pathways are associated with aging and longevity from yeast to mammals [11–14], reviewed in [15–19]. The insulin/insulin-like signaling (IIS) together with the target of rapamycin (TOR) pathways are among the most studied pathways. These pathways jointly regulate multiple metabolic processes affecting growth, reproduction, lifespan, and resistance to stress [20–22]. In insects, IIS/TOR signaling determines body size by coordinating nutrition with cell growth, and steroid and neuropeptide hormones to cede feeding when the target mass is attained [23]. Mutations that reduce IIS/TOR signaling reduce growth and reproduction, and increase stress resistance and lifespan [12, 24, 25]. Experimental evidence primarily from knockout studies suggest that IIS/TOR is a major coordinator of nutrient status with metabolic processes. For example, lack of nutrients blocks insulin production [26], resembles the effects of a down-regulated IIS/TOR [27], while a hyperactivated IIS/TOR pathway can exclude the necessity for nutrients [27]. Fruit flies raised on excess sugar diets as larvae become hyperglycemic, fat and insulin resistant, show increased expression of genes associated with gluconeogenesis, lipogenesis, β-oxidation, and

FOXO targets [8, 9]. Modulating TOR signalling slows aging by affecting downstream processes including mRNA translation, autophagy, endoplasmic reticulum stress signaling, stress responses, and metabolism (reviewed in [28]) .

Specific examples on the role of nutrient sensors abound in literature. Briefly, the forkhead transcription factor *foxo* in *Drosophila melanogaster (D. melanogaster)* and its orthologs in the nematode *Caenohabditis elegans* and vertebrates is the main transcription factor target of IIS, and is required for lifespan extension by a reduced IIS, reviewed in [18]. An activated *foxo* represses production insulin-like peptides (ILP) which in turn reduces IIS signaling [29, 30]. In a related mechanism, resveratrol-mediated activation of sirtuin genes mimic the effect of DR in promoting lifespan in many metazoans [1]. For example, in the cotton bollworm *Helicoverpa armigera Sirt2* extends lifespan by its role in cellular energy production and amino acid metabolism [31, 32]. Further, the regulation of appetite has a major effect on plastic nutrient allocation, reviewed in [33]. For example, leptin signaling together with the AMP-activated protein kinase (AMPK) affect nutrient intake and mediates production of ILPs [34–36]. Lastly, the hormones ecdysone and juvenile hormone also bear on the IIS to regulate ovary size and influence dispersal-reproduction trade-offs in *D. melanogaster* and sand crickets, *Gryllus firmus*, respectively *[21, 37–40]*, reviewed in [33]. In spite of these and other examples that demonstrate the effect of genetic variation on the metabolic response to nutrition, the underlying genetic basis diet effects in natural populations remain elusive [41].

Much of the current focus on how endocrine mechanisms affect phenotypic response to nutrition proceed in one-gene-at-a-time knockout strategies to elucidate function. This approach has been informative, largely in model species, but also supported to some extent in wild species. Thus, endocrine pathways can play a role in plastic and adaptive resource allocation in wild *D. melanogaster [42, 43]*, sexual selection of horn size in rhinoceros beetles [44], sex-specific mandible development in staghorn beetles [45, 46] morph determination in wing dimorphic sand crickets [38, 47–49] leading to the conclusion that endocrine pathways mediate the evolution of resource allocation strategies [50–52]. However, natural populations do not consistently reveal these same genetic mechanisms[53–56] suggesting that large effect studies in mutants

capture tails of effect distributions in the wild [57], or that different mechanisms overlapping with endocrine pathways may be involved [58, 59], reviewed in [33]. Presently, high-throughput genome-wide studies have become possible and cheaper, and generate high dimensional multi-level data from high replication experiments, allowing for a more comprehensive picture of these processes, providing the opportunity to integrate data types such as QTL and gene expression studies.

In this study, our goal is to understand the transcriptional response in different nutritional environments in a multiparent population. We use a synthetic population derived from the *Drosophila* Synthetic Population Resources (DSPR), and analyze RNA-seq data sequenced from pooled samples of female *D. melanogaster* exposed to multiple diet conditions differing in the proportion of protein and carbohydrate sources. We profile gene expression for three tissues in high replication, and ask:

1) How does gene expression change in response to nutritional environment?
2) What specific biological processes and pathways are significantly perturbed by diet treatment?
3) Which sets of genes show similar expression patterns across diets and tissues, and what biological processes are involved in these specific patterns?

Results

Global expression patterns

We sequenced total RNA from 54 samples comprising 18 samples each for DR, C, and HS diet treatments (Fig. 1). In each diet treatment, samples for three tissues (head, body and ovary) were collected in six replicates. An overview of transcripts across diets and tissues, transcript numbers per gene and transcript lengths is given in Figure 2. A total of 35,572 transcripts were obtained, out of which 18,678 transcripts remained for analysis after removal of transcripts with a variance across samples of less than one [60]. Overall expression levels were generally consistent across diet treatments and tissues (Fig. 2a. One sample (B2) in the DR treatment showed slightly lower median expression compared to the rest, but was similar enough to others and was retained in the analysis. The distributions of transcript counts, transcripts per gene, and transcript lengths in each sample are shown in Figures S1.

To assess global expression patterns over tissues and diets we performed principal components analysis (PCA) on all samples using an expression matrix from which batch effects had been removed (Fig. 2d). A similar figure prior to batch removal is shown in Figure S2. As expected, tissue effects strongly dominated variance in the first two components which jointly accounted for 97% of the total variance. PC1 which explains 72% of the variance in expression presents non-overlapping separation of tissue expression, although body and head expression appear somewhat similar compared to the ovaries. PC2 (25%) distinguishes expression in bodies from that in heads and ovaries. When organs are considered separately, diet effects become apparent, although they do not form non-overlapping clusters (Figure S3), reflecting the more subtle effect of diet when compared to the tissue effect.

Differential gene expression in response to diet

We used DESeq2 to quantify differential gene expression in head, ovary and body samples obtained from adult flies held on C, DR, and HS diet treatments. We obtained lists of genes significantly differentially expressed due to diet change overall (see model 3a). After filtering out genes with a low overall count, a total of 12,614 genes remained in the experiment based on which all subsequent results were obtained. Of these, 2,475 genes were differentially expressed in response to diet treatment, and 978 for the interaction between diet and tissue (LRT, adj. $P < 0.05$). These expression differences can be visualized for each tissue and diet pair in Figure 3. Overall, relative to the C diet, many genes in all organs were expressed in the same direction in the DR and HS diets, meaning that the genes that have decreased expression in DR tend to also have decreased expression in HS, and vice versa (Fig. 4 - see trend along dashed lines). This general trend is apparent in all tissues suggesting a similar change in global transcription in response to both the DR and HS diets relative to the C diet, despite their very different compositions and calorie content.

Gene set enrichment analysis

We performed gene set enrichment analysis (GSEA) on DEGs for the effect of diet (i.e. model 3a) for each diet-tissue combination to identify pathways and gene sets

which were significantly perturbed relative to all DEGs in the model. Of these pairwise comparisons, only DR versus HS in bodies and DR versus C in bodies showed evidence for significantly enriched gene sets/pathways at a q-value threshold of 0.05. We identified four pathways showing gene set level changes for bodies in DR relative to HS: dme01100: Metabolic pathways (two-sample t-test, mean change = 5.38, FDR q-value = $2.94e^{-06}$), dme01200: Carbon metabolism (two-sample t-test, mean change = 3.31, FDR = $2.26e^{-02}$), dme00190: Oxidative phosphorylation (two-sample t-test, mean change = 2.95, FDR = $4.52e^{-02}$), and dme04141: Protein processing in endoplasmic reticulum (two-sample t-test, mean change = 2.83, FDR = $4.52e^{-02}$). Notably, metabolic pathways (dme01100), which was most significantly enriched, is a large group of pathways in the KEGG database (https://www.genome.jp/kegg-bin/show_pathway?dme01100). At the default threshold (FDR $P_{adj.}$ <0.1) in GAGE, ten more pathways appeared for DR relative to HS in bodies. These additional pathways encompass three main metabolic themes: carbohydrate, amino acid and protein, and drug/xenobiotics (Table S3). For the comparison of DR versus C in bodies, oxidative phosphorylation (dme00190) was significantly enriched (two-sample t-test, mean change = 3.2, FDR $P_{adj.}$ = $7.36e^{-02}$). All pathways showing gene set perturbation showed positive regulation, with positive values in mean change which represents the magnitude and direction of gene-set level changes.

Further, we examined GO term enrichment for biological process (BP) to capture significant diet-related differences occurring below the level of pathway. Four terms were enriched at an FDR $P_{adj.}$ < 0.01: GO:0044281 small molecule metabolic process (mean change = 4.49) for the DR vs HS comparison in bodies; GO:0007154 cell communication (mean change = 5.10), GO:0023052 signaling (mean change = 5.06), and GO:0007165 signal transduction (mean change = 4.56), all for the HS vs C comparison in bodies. At an FDR $P_{adj.}$ < 0.05, 41 unique enriched terms were observed (Table S3). Of these, 34 terms for HS relative to C diet in heads highlighted several themes including signaling, metabolism, growth, cytoskeleton, gene expression and development. Three terms for HS relative to C in bodies included GO:0007154 cell communication, GO:0023052 signaling, and GO:0003008 system process. The remaining six terms were all for the HS diet relative to DR in bodies all within one theme

of metabolism (acid, small molecule, carbohydrate). No terms were enriched for the comparisons in ovaries. To understand broader inclusive processes represented by these GO terms, we evaluated our list for ancestral terms using QuickGO (EMBL-EBI https://www.ebi.ac.uk/QuickGO/). Nine terms at the same hierarchical level immediately below category BP were observed (metabolic process, biological regulation, cellular process, localization, response to stimulus, cellular component organization, multicellular organismal process, growth, and developmental process). Among these, GO:0008152 metabolic process, GO:0009987 cellular process, and GO:0032502 developmental process had the most connections to child terms. Our GSEA analysis therefore highlights multiple pathways and biological processes triggered by diet changes especially in bodies and heads, and encompassing broad themes from metabolism to signaling to homeostasis. Notably, our results do not show particular enrichment of diet-associated terms in ovaries, at least for biological processes.

Diet-induced gene coexpression

Next, we asked how diet treatment affected gene coexpression across tissues and diets. To identify coexpressed genes (or modules) we used gene expression profiles with batch effects removed (model 3a). Setting the minimum module size to 30 genes, a total of 31 modules were detected (range 39 - 3,240 genes), with 1,049 unassigned genes (grey module). After merging highly similar modules (i.e. eigengene correlation $r > 0.9$, see methods), 21 modules were identified with an additional module holding all unassigned genes (Table S4).

To appreciate module-level effects of diet and tissue on coexpression, we visualized eigengene expression across diets (Fig. 5, Table S4). It is clear from these plots that some modules showed greater interaction effects than others (e.g. *e*, *f*, *m*, *q*, *s* and *v*). These modules show either reduced or increased expression for one or two tissues in one or two diets. To gain better insight into these intra-modular effects of diet and diet-tissue interaction, we fit an analysis of variance model (ANOVA) to module eigengenes. For the effect of diet only (i.e. eigenegene ~ diet_tissue), all modules turned up significant (FDR $P_{adj.} < 0.05$), except modules *c* and *h* (Fig. 5). Similarly, for

the effect of the interaction between diet and tissue (i.e. eigenegene ~ diet * tissue),all modules showed a significant effect (FDR $P_{adj.} < 0.05$), except modules (*a*) and (*d*).

Focusing on the modules showing a statistically significant interaction effect, and divergent expression profiles in one or more diets for a given tissue (Fig. 5), several trends became apparent: 1) generally reduced expression in the DR diet for ovaries and bodies unlike the rest of diets (Fig. 5*e*, *k*, *f* and *s*), 2) increased expression in the DR diet for ovaries and bodies (*i*, *m*), and 3) elevated expression in bodies in both DR and HS diets (*v*), and 4) different responses in all three diets (*g*, *k*, *p*, *r*). An attempt to isolate specific diet-tissue combinations driving the interaction effect using *post hoc* tests revealed large numbers of highly significant combinations. We therefore explored the modules further via functional enrichment to identify the processes driving these coexpression patterns.

We conducted functional analysis on all modules to identify enriched GO terms (Bonferroni corrected enrichment *P* values, Table S5). Of 12,614 entrez identifiers in our experiment, 10,334 mapped in current GO categories using the package GO.db, and therefore used as a background list for enrichment analysis in WGCNA. Removal of weakly assigned genes identified by resampling did not affect the outcome as terms did not change between the two analyses. A large number of terms were obtained across CC, MF and BP categories: 658 terms ($P < 0.01$), and 791 terms (Bonferroni corrected $P < 0.05$) (Table S5). A visual inspection of enriched terms in the 21 robustly assigned modules, revealed a large diversity of biological processes, ranging from nuclear processes, to membrane and cytosolic processes; from structural to signaling and immune response processes; and from pigmentation to homeostatic processes.

The first module (Fig. 5*a*) which included 2,956 showed 291 GO terms (Bonferroni corrected, $P_{adj.} < 0.01$), and had the most significantly enriched terms (i.e. >60 terms ranged between $P_{adj.} < e^{-156}$ - $<e^{-15}$). This module was characterized by greater eigengene expression in ovaries compared to heads and bodies, although the diet effect was subtle but significant. Nuclear and intracellular organelle processes including gene expression, and RNA processing were key tissue (ANOVA, $P < 2e\text{-}16$) and diet (ANOVA, $P < 0.002$) effects independently regulated (i.e. no interaction effect). With reference to the trends described above (Fig. 5), those modules showing generally

reduced expression in the DR diet for ovaries and bodies (*e*, *k*, *f* and *s*), are associated with biological processes including signaling (*e*, $P_{adj.}$ <1.1e^{-10}), cellular component organization (*k*, $P_{adj.}$ <5.8e^{-09}), nervous system development (*f*, $P_{adj.}$ <1.3e^{-14}), signaling and protein localization on Golgi apparatus (*s*, $P_{adj.}$ <3.0e^{-06}). Interestingly, expression increase in DR in bodies and heads compared to ovaries is related to ubiquitin-dependent proteolytic processes in the proteasome (*i*, $P_{adj.}$ <1.8e^{-08}), and cytosolic vesicle transport/mitochondrial activities (*m*, $P_{adj.}$ <8.9e^{-156}). Module (*v*, $P_{adj.}$ <1.1e^{-21}) was interesting because bodies show monotonic increase in expression from C to DR to HS, a trend that may relate to the GO term chitin-based cuticle development.

Analysis of our modules therefore revealed a large number of biological processes (BP), molecular function (MF) and cellular components (CC) (Table S5); a large tissue effect (Fig. 2*d*), significant diet and interaction effects; reduced expression for signaling activity in the DR diet ; increased expression for catabolic processes in the DR diet; and increased expression in non-C diets for cuticular remodeling (Fig. 5). These results suggest that response to diet changes in natural *D. melanogaster* involves multi-system response rather than one or a few signaling pathways that can be very different in different tissues.

Parsing previously identified QTL for the response to diet

A useful application of genome-wide expression data is to identify possible regulatory variants underlying QTL. In a previous study, we used a multivariate approach to identify a global expression QTL for the response to diet treatment of 52 genes in the IIS/TOR pathways [61] that we hypothesized was influencing the expression of many of the genes in these pathways. After performing a discriminant function analysis predicting diet (DR or C) from expression measured on whole flies of 52 genes in the IIS/TOR pathways, we mapped the difference in discriminant function to identify this eQTL. The eQTL interval, as defined by the Bayesian credible interval, contains 327 genes, making it challenging to narrow to possible candidates. We therefore searched for differentially expressed genes identified in this study that fall within this eQTL region of interest. Of these, we find 49 genes are differentially expressed in the different diet treatments and 13 show a diet by tissue interaction, with

5 of these genes showing both a main treatment effect and an interaction effect. The patterns of expression across tissues for this set of genes is shown in Figure 6. While our expression results don't allow us to narrow to a single candidate, they do significantly reduce the list and provide detailed expression data for the possible causal genes.

Previously implicated pathways

Several pathways have been well-studied in the context of diet-induced phenotypic changes. We specifically examined these pathways in order to characterize the transcriptional response. We obtained a precomputed list of genes for key metabolic pathways (fbgn_annotation_ID_fb_2019_02.tsv): IIS (55 genes), TOR (152 genes), and FOXO (110 genes, which includes the *Sir* genes). Of 317 pathway genes, 315 were present in modules resulting from hierarchical clustering, out of which 47 were significantly differentially expressed for the diet effect. Our GSEA results presented above did not show pathway level enrichment of any of these pathways as defined in KEGG Pathway Database (https://www.genome.jp/kegg/pathway.html), although as mentioned above, a handful of member genes were differentially expressed. These genes that were differentially expressed however, showed mixed modular membership in our clustering results. Similarly, GO analysis on module genes did not enrich categories specifically including 'insulin', 'TOR' and 'FoxO' in the term. In this regard, five terms present in our data were not significantly enriched (Fisher exact test, *P-adj*. > 0.05), and no term at all was present for FoxO. From these results we could not link any of these pathways with particular modules within our data. Importantly, we did not find evidence for significant whole pathway perturbation of IIS/TOR and the downstream FOXO signaling in our coexpressed modules.

Discussion

We sequenced pooled RNA samples from a three-diet by three-tissue by six-replicate experiment of outbred mated female *D. melanogaster* in the DSPR. Our aim was to understand diet-induced patterns of gene expression influencing plastic nutrient allocation in different diet conditions in a multiparent population resource. Our results

suggest that: 1) global expression patterns are dominated by tissue and diet-tissue interaction effects, while the effects of diet alone are subtle but significant, 2) patterns of gene expression are generally similar in low-protein and carbohydrate-rich diets relative to the control diet, 3) multiple pathways, coexpressed gene modules, and biological processes are invoked that affect transcription in different diet conditions, especially in the head and body tissues, and 4) expression results did not suggest a single regulatory variant underlying QTL, but narrowed down to a few possible causal genes. Overall, our results suggest that multiple networks are involved in phenoypic changes in response to nutrient availability, rather than just a few key genes. We advocate a broader, genome-wide approach to studying the genetic mechanisms underlying how diet affects phenotypic change.

It is established that nutrient signaling pathways and hub genes in those pathways play a crucial role in how organisms adjust to changing conditions in availability and quality of nutrients to optimize fitness traits. Analysis of differential gene expression in a genotype presented with diets differing in nutritional richness provides an 'omic' alternative to study intermediate processes that connect genetic architectures to phenotypic outcomes such as allocation patterns. In fruit flies, studies typically focus on whole-body or head tissue transcription (e.g. [62]); one or a few gene pathways known to affect diet responses at a time (e.g. [61]); one or two diet manipulations (e.g. [62–64]), but scarcely integrate over more than two organs and conditions at a time, or explore outside a few gene pathways. Further, despite costs trending downwards recently, sequencing of more highly replicated experiments remains unaffordable for many laboratories. By and large, studies in model organisms focus on genes in a few endocrine pathways, so called nutrient sensors, as critical players in coordinating growth, reproduction, and somatic maintenance responses to changing diet conditions. Components of the IIS/TOR, growth, and ecdysone hormones; and sirtuin deacetylases are deemed some of the major players in this respect. Our results suggest an expanded scope of mechanisms underlying flexible responses to nutrient limitation (DR studies) or oversupply (high sugar and high fat diet studies) in natural populations, which has also been suggested by. We discuss our major results and their implications below.

First, we observed a large global effect of tissue type and a more subtle, but significant, effect of diet treatment. Previous studies in flies have also found relatively small effects of diet on transcription. Previously, we characterized the genetic basis of standing genetic variation for 55 genes of the IIS/TOR pathway following treatment with the same diets used here [61], and found only small changes in gene expression associated with diet treatment although most of those genes were differentially expressed. Similarly, Reed et al, [65] measured transcriptional and metabolomic changes for 20 inbred lines (North Carolina and Maine population) of *D. melanogaster* treated with four diets varying in sugar and fat content and observed a small dietary component in gene expression profiles, with much larger contributions of genotype by diet interactions. Musselman et al. [66] investigating expression differences in *D. melanogaster* fed with two different forms of sugar found small but significant changes in gene expression. Overall, diet seems to produce fairly small magnitude changes in expression in many genes across the genome, which in concert presumably can lead to large phenotypic changes.

Secondly, comparisons between DR and HS diets relative to C revealed a similar pattern of expression. This result mirrors our earlier finding [61] in which gene expression in DR and HS relative to C generally trended in the same direction. This result is in spite of the fact that the DR and HS diets lead to very different outcomes in median lifespan and fecundity in our population [61, 67]. Nutritional geometry studies which measure traits in a series of concentrations of liquid media suggest that traits such as lifespan and reproduction (which differ significantly across our diets) are influenced primarily by the diet protein to carbon (P:C) ratio, not its caloric content (e.g., [8, 68, 69]. Thus calorie limitation alone does not drive phenotypic patterns in these studies. While our HS diet has a high concentration of sugar per liter of food, the P:C ratio is low (i.e. ~1:2 yeast to sugar ratio). Lifespan and fecundity in nutritional geometry studies are maximized at a much lower P:C ratio (i.e. 2- to 4- lower than our HS diet) [68, 69]. Thus our results are consistent with similarity in expression pattern between DR and HS. It is also possible that diet macromolecules serve only as a cue that lead to optimal allocation of resources in natural populations. Thus, it is possible for expression measures to trend in the same direction in DR and HS. Further, Dobson et al. [70] found

that excess sugar diets in young adult flies inhibited *foxo* and reduced survival in middle and old age. While we did not measure lifespan and fecundity here, our data showed mixed pattern of *foxo* activation in across diet tissue combinations, and these mapped to many coexpression modules (Table S5) which may be due to the relatively young age (i.e. 21 days) of our experimental flies.

Thirdly, an overall take away from our GSEA on the full dataset, and also on gene modules coming from hierarchical clustering was that diet effects could not be attributed to a particular genetic mechanism. GSEA highlighted metabolism, oxidative phosphorylation and protein processing at pathway level, but showed a broad spectrum of processes in GO analysis encompassing metabolism, cell signaling, structural development and organization, and defence. Similarly, GO analysis of gene modules yielded a broad range of biological processes. From both these analyses, IIS, TOR, and FOXO signaling were not significantly enriched. However, several genes had significantly reduced expression in the IIS/TOR (e.g. *Ilp5*, *Rheb*, *Atg1*, *Myc*, and *eIF4E1*) and significantly higher expression in FoxO downstream effectors (e.g. *AMPK, orct2*, *Gadd45, cdk2* and *p38*) in most DR-tissue combinations consistent with indicating canonical activity. With the exception of *Ilp5 [41]* however, undetectable differential expression of hub genes (such as *Ilp2, S6K*, *chico, InR, Akt1, Torc, Thor, and foxo*) suggest that diet induced more pathways/genes than the focus in the field currently is.

Evidence in *C. elegans* suggest that the worm ortholog of *foxo*, *daf-16* is not required in the DR response [71–74]. On the other hand, *sir-2.1* is a worm ortholog of the fruit fly *sirt 2* (for which expression was increased in all tissue-diet combinations in this study), and is required for lifespan extension in adult worms by diet deprivation was independent of the *daf-2*/insulin-like signaling [74]. In *D. melanogaster*, similar evidence is emerging that suggest is not required for the response to DR [75], but is involved in the normal response to DR [76]. When *dFOXO* was removed, DR treatment still resulted in significant lifespan extension in null flies [75]. Another study testing a novel DR assay in *C. elegans* found that DAF-16, but not DAF-2 (the worm lnR) was required when DR was performed on solid media, and concluded that AMPK-FOXO signaling resulted in lifespan extension on solid food [77]. Our data provides further evidence

supporting these studies in suggesting a broader mechanism in which IIS, TOR and FOXO play a role, but in concert with other pathways.

Our data certainly includes heterogeneity in tissue types which may affect the level and nature of gene expression [84]. For instance, fewer cell types likely in the ovaries and head compared to body samples may affect the range of biological processes that get triggered by nutrient levels. Further, DR and HS methods vary tremendously across laboratories such different methods affect different subsets of nutrient pathways [75]. Patterns of phenotypic expression (fecundity and lifespan) and patterns of gene expression have held stable across several studies in our population, suggesting that the effects we find are biologically relevant in the DSPR.

In conclusion, we find that a diverse set of pathways, gene networks and biological processes are involved in the response to nutritional changes in a multiparent population. We urge for more multilevel, multi-system approaches to nutrigenomic studies in addition to the more targeted approaches that are commonly in use.

Methods

Experimental population

We used 835 recombinant inbred lines (RILs) of the *p*B sub-population of the *Drosophila* Synthetic Population Resource, DSPR [85, 86] as source of our experimental population. Five young females that had mated intra-line were randomly selected from each RIL and placed in six custom-made cages each measuring 20.3 cm x 20.3 cm x 20.3 cm. Eggs were collected (twice on successive days) after 22 hours of oviposition in milk bottles (250 ml) containing 40 ml media. Resulting flies were introduced to six cages in large population sizes (i.e. > 2000 per cage) and allowed to mate for five generations (21-day cycle). To ensure a genetically homogenous base population was generated, eggs from each cage equally seeded each of the 5 other cages at each generation. We refer to these six cages as the base population. All life stages during generation of the base population were reared on a cornmeal-dextrose-yeast maintenance diet. Proportions of ingredients in our maintenance diet are presented in Table S1. Additional culture practices including equipment and supplies are described in Ng'oma *et al*, [87].

Study design

We used one random cage from the base population for phenotyping to generate RNA-seq data we present here. This population is referred to as the "synthetic population". We adopted a factorial design comprising three dietary treatments, three tissues, and six replicates per each treatment-tissue combination. To obtain flies for each diet treatment, we placed two plates (100mm x 15 mm, Fisherbrand®) of maintenance diet in the synthetic population and allowed for 24 hours of oviposition, repeating egg collection three times. From the two egg plates, a thin slice of media bearing 50 - 90 eggs (visually estimated) was cut out and grafted to each of 60 new vials (25 mm x 95 mm, Polystyrene Reload, cat. no. 32—109RL, Genesee Scientific, USA) of maintenance food containing 10 ml media. At 12 days post-oviposition, eclosed flies were released into 9 cages, 3 cages for each of three diet treatments, such that treatments are equally represented across egg collection dates. For each cage, we used 20 vials to seed the cage with adult flies. Flies were held on treatment diet for 10 days, and provided with new food every 2 - 3 days. Each replicate was started on a new week to provide for time that would be needed to dissect a large number of flies per replicate later on. All flies were reared in a growth chamber at 23 □C, ≥50% relative humidity, and a 24:0 light:dark cycle, which are the typical maintenance conditions for the DSPR flies. Details of our study design are schematically shown in Fig.1.

Experimental diets

We extracted RNA for sequencing from 22 day-old (post-oviposition) female flies held on three experimental diets adapted from Bass *et al*, [88] and Skorupa *et al*, [8]: control (C), dietary restriction (DR), and high sugar (HS) for 10 days, as described above. These are all cornmeal-sucrose-yeast diets which differ in two ways: relative to C, DR contains 50% less yeast, and HS contains about seven times sucrose (Table S1). We have used these diets in past studies to map expression QTL in the DSPR RILs [61], and to estimate quantitative genetic parameters in an outbred DSPR population (Ng'oma et al, 2018). To prevent desiccation and preserve quality, diets were covered with multipurpose sealing wrap (Press'n Seal®) sealed and stored at 4 □C and used within 2 weeks of preparation. To prevent food degradation, individuals were moved to vials with fresh food three times per week.

Sample preparation and sequencing

At day 22, we collected 100 - 104 females per diet treatment under mild CO_2 anesthesia. We replicated this process six times over six days, thus creating six same-age sample batches with each batch including all three treatments (Table 2b). This yielded assays of at least 100 females per treatment diet (HS, C and DR), three tissues within each diet (heads, ovaries and bodies), biologically replicated 6 times. Our experiment therefore comprised 54 samples (18 per diet). We immediately dissected tissues from these females and promptly flash-froze them in liquid nitrogen and held them in a closed styrofoam box on dry ice before storage at -80 ^{o}C. Precision scissors (RS-5604, Roboz Surgical Instrument Co., Inc.) were used for fly dissection in a bath of pH 7.4, 1% PBS (Life Technologies™) containing 2 drops (80-100 µl) Triton x100 (SIGMA) under dissecting stereoscopes (Leica S6E and Leica M216) in 100 mm x 15 mm polystyrene petri dishes (Fisherbrand®). Scissors and forceps were rinsed with 70% ethanol and wiped dry with Kimwipes between samples. To minimize time-of-day effects, dissection was done across treatments (e.g. [C, HS, DR], [DR, HS, C], etc) rather than one treatment at a time (e.g. [C, C, C], [HS, HS, HS], etc).

We purified whole RNA from each of 54 samples using a protocol modified from Life Technologies TRIzol RNA extraction protocol. Tissues were homogenized in a tissue lyser using steel beads in 1 ml TRIzol reagent, and subsequent RNA extraction by following the TRIzol protocol. RNA quality was evaluated on a Nanodrop 2000 spectrophotometer (Thermo Scientific) and concentration on a Qubit 2.0 fluorometer (Invitrogen, Life Technologies). An additional clean-up step with a QIAGEN RNeasy Plus Mini Kit (Hilden, Germany) was used for gDNA elimination following manufacturer's protocol to achieve high quality RNA for library preparation. After the RNA cleaning step, yields typically ranged between 400 - 800 ng/µl; and absorbance values (260/280 and 260/230) above 2.0 (Table S2a). Fifty-four libraries were each prepared from 1.5 µg total mRNA, RNA integrity (RIN) ≥ 8.0 using Illumina's TruSeq Stranded mRNA (poly A enrichment) and single-end read sequencing on Illumina HiSeq 500. Barcoded libraries were combined in a single 54-plex library, which we sequenced on three lanes of a NextSeq 1x75 bp run to obtain ~20 million reads per sample (average: 23 million reads

per sample). The resulting reads were trimmed of adaptor sequences and FASTQC was used to assess quality. Sequencing was performed at the University of Missouri DNA Core Facility.

Data analysis

Read alignment and quantification of expression

We employed the 'new Tuxedo' suite analysis pipeline [60] for read assembly and transcript quantification. We mapped single-end reads to the reference genome of *D. melanogaster*, bdgp6_tran (ftp://ftp.ccb.jhu.edu/pub/infphilo/hisat2/data/, updated March, 2016,), using HISAT2 (version 2.1.0, Kim *et al*, [89]. Alignments were converted to BAM file format and runs combined using SAMtools [90]. Then, StringTie [60, 91] was used to assemble RNA-seq alignment into full-length transcripts, and to quantify levels transcript expression.

We intended our downstream analysis to focus on gene-level differential expression of known genes in the *D. melanogaster* transcriptome. Therefore we used the alternative workflow given by Pertea et al [60] skipping steps 3 - 5 in that protocol, (i.e. we skipped the individual assembly of each sample and the merge step, documented here http://ccb.jhu.edu/software/stringtie/index.shtml?t=manual#de, last accessed May 20, 2019). To do this, we ran 'stringtie -eB' directly on the output of 'samtools -sort'. In order to extract more gene (FBgn) ids from reference gene annotations into StringTie output, we ran a Perl post-processing script, '*mstrg_prep.pl*' (Pertea, https://gist.github.com/gpertea/b83f1b32435e166afa92a2d388527f4b) that appends reference gene ids to the MSTRG gene ids used in StringTie. In order to perform differential expression analysis on row counts using DESeq2 [92], we processed the output from StringTie with a Python script '*prepDE.py*' (Pertea M, http://ccb.jhu.edu/software/stringtie/index.shtml?t=manual#de) with the -e parameter to extract read count matrices (one for transcripts, one for genes) directly from the files generated by StringTie.

Controlling for batch effects

As described earlier, our samples were processed in six groups on separate days (all treatments and tissues represented equally in each) including setup, dissection, and RNA extraction and preparation (Table 2a). We sought to control for this obvious batch effect and any unknown underlying batch effects. We therefore used surrogate variable analysis (SVA, [93] implemented in the R library svaseq [94]. We used the DEseq2 package [92] to obtain counts that are normalized for library size (i.e. counts divided by size factors). Eliminating genes with zero counts, we used the svaseq function comparing a model with a known batch: mod ~treatment*[tissue+batch] to a null model with batch mod0 ~batch. A single surrogate variable (SV) was identified and included in all subsequent models.

Differential gene expression

Next, we estimated differential gene expression with DESeq2 for DR and HS treatment conditions relative to the C treatment. We fit two generalized linear models (GLM), henceforth called DESeq models, with parameter fitType = 'local' and only genes with at least 10 reads in at least 2 samples. First, we modeled the effect of diet treatment on differential expression while accounting for tissue and batch effects additively:

design ~SV1 + batch + tissue + treatment, (1)

where SV1 is the SV identified earlier. The second DESeq model considered the interaction effect of tissue with diet treatment,

design ~SV1 + batch + tissue * treatment. (2)

We used the likelihood ratio test to compare these two models [92] and obtain the genes significantly differentially expressed due to diet and tissue, respectively:

reduced=~ SV1 + batch + treatment (3a)

reduced=~ SV1 + batch + tissue (3b)

From these models we identified sets of differentially expressed genes (DEGs) which we analyze further after applying variance shrinkage to estimate fold change between conditions and within-group variance [92]. To identify global patterns of expression across diets and tissues, we performed a principal components analysis (PCA) on expression values before and after removal of batch effects.

Gene set enrichment in relation to diet

We considered our list of DEGs for the effect of diet treatment (model 1) and used the R Bioconductor GAGE package [95] to infer gene sets and pathways that were significantly perturbed relative to all DEGs. Briefly, GAGE takes an expression matrix with log-based fold changes as input. It assumes that a particular gene set or canonical pathway (from literature or database) comes from a different distribution than the experiment-derived background list. Therefore a two-sample t-test is applied to account for the gene set specific variance and the background variance and derives 1) a global p-value using a meta-test on p-values from gene set comparisons, and 2) a FDR q-value adjustment using Using GAGE to access the Fly annotation database 'org.Dm.eg.db', we generated up-to-date KEGG (Kyoto Encyclopedia of Genes and Genomes [96]) pathway gene sets, limiting our search to metabolic and signaling functional annotations. Similarly, we obtained up-to-date gene ontology (GO) gene sets specifying biological processes. We mapped our FlyBase gene (FBgn) IDs to ENTREZ ids, and performed pathway and gene set enrichment, and GO analysis on the resulting gene list within GAGE with the gage() function. We tested for perturbation of each gene set relative to all genes in the experiment by calculating the mean individual statistics (stat.mean) from multiple gene set tests using a two-sample t-test implemented in GAGE as gs.tTest(), and obtain a global p-value from individual p-values. The global p-values were then adjusted for multiple testing using the Benjamini & Hochberg procedure [97], and refer to these as FDR q-value [95].

Gene co-expression analysis

Next, we sought to identify sets of genes (modules) showing high correlation in their pattern of expression across tissues with respect to treatment condition. We used the removeBatchEffect() in the R limma package to correct for known (batch) and identified (SV1) effects. We applied a regularized log transformation (rlog) to the batch-corrected matrix to minimize differences between samples for rows with low counts as well as normalize to library size. The rlog transformation is recommended if, as in this study (0.52 - 1.92), size factors vary widely [92]. The resulting expression matrix was

used as input in the R package, Weighted Gene Co-expression Network Analysis, WGCNA, [98] to identify coexpressed gene modules showing similar patterns of expression across tissues and treatments. We built the initial network from samples over all treatments (N = 54) using a signed adjacency matrix with power 23 (i.e. function pickSoftThreshold()) to construct the topological overlap matrix (TOM) from all 12,614 genes (see results). This power represents the lowest power for which the scale-free topology fit index curve flattens out after reaching a high value of $r^2 = 0.90$. We performed hierarchical clustering of the TOM using the flashClust() function (method = "average") which implements hclust() clustering more efficiently for large datasets [99]. We used the cutTreeDynamic() function to identify initial the initial set of modules at the following thresholds: cutHeight = 0.95 (default), deepSplit = 2, minClusterDendro = 30, pamRespectsDendro = FALSE. A module eigengene is defined as the first principal component of a given set of co-expressed genes, and can be considered as a representative of the gene expression profiles in that set [98]. By convention, modules are referred to by their color labels, and, the grey module is used by default to contain genes not assigned to any module [100].

We then evaluated module membership using a resampling strategy described in Sikkink et al, [101]. Randomly, we chose four of six replicates for each diet-sample combination to produce 100 new datasets, each with 36 samples. Using the same parameters as in the full dataset, WGCNA was re-run for each new dataset and resulting modules examined for gene membership. First, a resampled module was accepted if it included at least 10% of the genes in the corresponding module in the full dataset. Secondly, a gene was considered to be strongly supported to belong to a module in the full dataset if it appeared in that module in at least 50% of resampled networks. We identified genes that failed to meet these criteria and placed them in the unassigned module. e merged highly correlated modules (r 0.9) during network construction for each resampled dataset to be consistent with how the full dataset was analyzed.

To summarize major patterns of within-module expression with respect to diet condition, we extracted the first principal component of expression of genes in each module, called the module eigengene. We then performed an ANOVA for each module

eigengenes to assess the effects of diet, tissue, and diet-tissue interactions on total module expression. Because many modules had a significant effect of either diet or diet-tissue interaction, we could not perform *post-hoc* tests to identify pairwise differences between diet treatments, preferring instead to examine module enrichment for diet-related functional annotations. We therefore accessed Bioconductor annotation libraries AnnotationDbi and org.Dm.eg.db using the GOenrichmentAnalysis() function within WGCNA, and calculated the Fisher's Exact test with the Bonferroni correction to identify significantly enriched GO terms in each module, providing all genes available in our experiment as a background list. We reviewed all terms significantly enriched ($P_{adj.} < 0.01$) for the BP category (to view terms for CC, MF, see Table S5).

Acknowledgements

We would like to acknowledge Elizabeth Lo Presti, Michael Reed, and Kevin Middleton for help with experimental setup and fly husbandry. High-throughput sequencing services were performed at the University of Missouri DNA Core Facility. The computation for this work was performed on the high-performance computing infrastructure provided by Research Computing Support Services and in part by the National Science Foundation under grant number CNS-1429294 at the University of Missouri, Columbia Mo. Funding for this study was provided by NIH R01 GM117135 and NSF IOS 1654866 to E.G.K.

Figure captions

Figure 1: Study design. Flies drawn from 835 RILs of the DSPR were bred together for 5 generations to create an outbred panel. Eggs were collected from this homogenous population and resulting flies reared on dietary restriction (DR), control (C) and high sugar (HS) diets in six replicates for 10 days from day 12 post-oviposition. Heads, ovaries and bodies were dissected over 100 female flies from each treatment replicate for total mRNA extraction.

Figure 2: Global patterns of gene expression in 54 RNA samples. **a.** Transcript abundance as $\log_2$(FPKM + 1) for each sample (x-axis: bodies, B1 - B6 ; heads, H1 -

H6; and ovaries, O1 - O6), and diet C, DR, and HS. **b.** Distribution of transcripts per gene - the number of transcripts associated with each gene symbol. **c.** Distribution of transcript sizes - based on transcript models of annotated genes. FPKM - Fragments Per Kilobase Million. **d.** Principal components analysis (PCA) to visualize the overall effect of diet and tissue. Two dimensions are shown (PC1 and PC2).

Figure 3: Comparison between DR and HS fold change. Horizontal and vertical lines at 0 show when gene expression in the two diets is the same relative to the C diet. Diagonal dashed line is the 1:1 line. Points in the quadrants above 0 for one diet and below 0 for the other are genes that trend in different directions in the HS vs. DR diet relative to C (top-left and bottom-right). Points falling above the 1:1 line in the top-right quadrant and below the 1:1 line in the bottom-left quadrant show a similar effect in the HS diet as in the DR diet. Points are colored according to their mean expression.

Figure 4: Volcano plots (**a - i**) for differentially expressed genes showing genes with large fold changes that are also statistically significant. Horizontal lines indicate - $\log_{10}$(P.adj) = 0.05, and points above the line represent genes with statistically significant differential expression. Vertical lines differential expression with the value of $\log_2$ fold change of 1 (i.e. absolute fold change = 2) and FDR = 0.05. Upregulated and downregulated genes are on the right side and left side of the vertical lines, respectively, and statistically significant genes are above horizontal lines. Rows in the panel top to bottom are bodies, heads, and ovaries; columns left to right are DR vs C, HS vs C, DR, vs HS; color of points represent $\log_{10}$ of base mean expression.

Figure 5: Eigenegene expression across diet treatment for each module *a* - *v* identified in hierarchical clustering. Color scheme represent the three diets; each filled circle represents a sample; the open triangle marks the mean eigene expression for a given diet in a given tissue. Red, bodies; blue, ovaries; green, heads.

References

1. Wood JG, Rogina B, Lavu S, Howitz K, Helfand SL, Tatar M, et al. Sirtuin activators mimic caloric restriction and delay ageing in metazoans. Nature. 2004;430:686–9.

2. Sohal R, Weindruch R. Oxidative stress, caloric restriction, and aging. Science. 1996. http://www.sciencemag.org/cgi/content/abstract/sci;273/5271/59.

3. Shanley DP, Kirkwood TB. Calorie restriction and aging: a life-history analysis. Evolution. 2000;54:740–50.

4. Sinclair DA. Toward a unified theory of caloric restriction and longevity regulation. Mech Ageing Dev. 2005;126:987–1002.

5. Neel JV. Diabetes mellitus: A “thrifty” genotype rendered detrimental by “progress”? Am J Hum Genet. 1962;14:353–62.

6. Wells JCK. Thrift: a guide to thrifty genes, thrifty phenotypes and thrifty norms. Int J Obes . 2009;33:1331–8.

7. May CM, van den Heuvel J, Doroszuk A, Hoedjes KM, Flatt T, Zwaan BJ. Adaptation to developmental diet influences the response to selection on age at reproduction in the fruit fly. J Evol Biol. 2019;32:425–37.

8. Skorupa DA, Dervisefendic A, Zwiener J, Pletcher SD. Dietary composition specifies consumption, obesity, and lifespan in Drosophila melanogaster. Aging Cell. 2008;7:478–90.

9. Musselman LP, Fink JL, Narzinski K, Ramachandran PV, Hathiramani SS, Cagan RL, et al. A high-sugar diet produces obesity and insulin resistance in wild-type Drosophila. Dis Model Mech. 2011;4:842–9.

10. Na J, Musselman LP, Pendse J, Baranski TJ, Bodmer R, Ocorr K, et al. A Drosophila model of high sugar diet-induced cardiomyopathy. PLoS Genet. 2013;9:e1003175.

11. Tatar M, Post S, Yu K. Nutrient control of Drosophila longevity. Trends Endocrinol Metab. 2014;:1–9.

12. Kapahi P, Zid BM, Harper T, Koslover D, Sapin V, Benzer S. Regulation of lifespan in Drosophila by modulation of genes in the TOR signaling pathway. Curr Biol. 2004;14:885–90.

13. Bolukbasi E, Khericha M, Regan JC, Ivanov DK, Adcott J, Dyson MC, et al. Intestinal Fork Head Regulates Nutrient Absorption and Promotes Longevity. Cell Rep. 2017;21:641–53.

14. Essers P, Tain LS, Nespital T, Goncalves J, Froehlich J, Partridge L. Reduced insulin/insulin-like growth factor signaling decreases translation in Drosophila and mice. Sci Rep. 2016;6:30290.

15. Giannakou ME, Partridge L. Role of insulin-like signalling in Drosophila lifespan. Trends Biochem Sci. 2007;32:180–8.

16. Kaletsky R, Murphy CT. The role of insulin/IGF-like signaling in C. elegans longevity and aging. Dis Model Mech. 2010;:1–5.

17. Teleman AA. Molecular mechanisms of metabolic regulation by insulin in Drosophila. Biochem J. 2010;425:13–26.

18. Partridge L, Alic N, Bjedov I, Piper MDW. Ageing in Drosophila: the role of the insulin/Igf and TOR signalling network. EXG. 2011;46:1–6.

19. Kapahi P, Kaeberlein M, Hansen M. Dietary restriction and lifespan: Lessons from invertebrate models. Ageing Res Rev. 2017;39:3–14.

20. Kenyon C, Chang J, Gensch E, Rudner A, Tabtiang R. A C. elegans mutant that lives twice as long as wild type. Nature. 1993;366:461–4.

21. Tatar M, Kopelman A, Epstein D, Tu MP, Yin CM, Garofalo RS. A mutant Drosophila insulin receptor homolog that extends life-span and impairs neuroendocrine function. Science. 2001;292:107–10.

22. Clancy DJ, Gems D, Harshman LG, Oldham S, Stocker H, Hafen E, et al. Extension of life-span by loss of CHICO, a Drosophila insulin receptor substrate protein. Science. 2001;292:104–6.

23. Edgar BA. How flies get their size: genetics meets physiology. Nat Rev Genet. 2006;7:907–16.

24. Vellai T, Takacs-Vellai K, Zhang Y, Kovacs AL, Orosz L, Müller F. Genetics: influence of TOR kinase on lifespan in C. elegans. Nature. 2003;426:620.

25. Hansen M, Taubert S, Crawford D, Libina N, Lee S-J, Kenyon C. Lifespan extension by conditions that inhibit translation in Caenorhabditis elegans. Aging Cell. 2007;6:95–110.

26. Géminard C, Rulifson EJ, Léopold P. Remote control of insulin secretion by fat cells in Drosophila. Cell Metab. 2009;10:199–207.

27. Britton JS, Lockwood WK, Li L, Cohen SM, Edgar BA. Drosophila's insulin/PI3-kinase pathway coordinates cellular metabolism with nutritional conditions. Developmental Cell. 2002;2:239–49. doi:10.1016/s1534-5807(02)00117-x.

28. Kapahi P, Chen D, Rogers AN, Katewa SD, Li PW-L, Thomas EL, et al. With TOR,

Less Is More: A Key Role for the Conserved Nutrient-Sensing TOR Pathway in Aging. Cell Metab. 2010;11:453–65.

29. Giannakou ME, Goss M, Jünger MA, Hafen E, Leevers SJ, Partridge L. Long-lived Drosophila with overexpressed dFOXO in adult fat body. Science. 2004;305:361.

30. Hwangbo DS, Gersham B, Tu MP, Palmer M, Tatar M. Drosophila dFOXO controls lifespan and regulates insulin signalling in brain and fat body. Nature. 2004;429:562–6.

31. Rahman M, Nirala NK, Singh A, Zhu LJ, Taguchi K, Bamba T, et al. Drosophila Sirt2/mammalian SIRT3 deacetylates ATP synthase β and regulates complex V activity. J Cell Biol. 2014;206:289–305.

32. Wang T, Geng S-L, Guan Y-M, Xu W-H. Deacetylation of metabolic enzymes by Sirt2 modulates pyruvate homeostasis to extend insect lifespan. Aging. 2018;10:1053–72. doi:10.18632/aging.101447.

33. Ng'oma E, Perinchery AM, King EG. How to get the most bang for your buck: the evolution and physiology of nutrition-dependent resource allocation strategies. Proc Biol Sci. 2017;284. doi:10.1098/rspb.2017.0445.

34. Hardie DG, Ross FA, Hawley SA. AMPK: a nutrient and energy sensor that maintains energy homeostasis. Nat Rev Mol Cell Biol. 2012;13:251–62.

35. French SS, Denise Dearing M, Demas GE. Leptin as a Physiological Mediator of Energetic Trade-Offs in Ecoimmunology: Implications for Disease. Integr Comp Biol. 2011;51:505–13.

36. Rajan A, Perrimon N. Drosophila cytokine unpaired 2 regulates physiological homeostasis by remotely controlling insulin secretion. Cell. 2012;151:123–37.

37. Zera AJ. Intermediary metabolism and life history trade-offs: lipid metabolism in lines of the wing-polymorphic cricket, Gryllus firmus, selected for flight capability vs. early age reproduction. Integr Comp Biol. 2005;45:511–24.

38. Zhao Z, Zera AJ. Biochemical basis of specialization for dispersal vs. reproduction in a wing-polymorphic cricket: Morph-specific metabolism of amino acids. J Insect Physiol. 2006;52:646–58.

39. Toivonen JM, Partridge L. Endocrine regulation of aging and reproduction in Drosophila. Mol Cell Endocrinol. 2009;299:39–50.

40. Efeyan A, Comb WC, Sabatini DM. Nutrient-sensing mechanisms and pathways. Nature. 2015;517:302–10.

41. Min K-J, Yamamoto R, Buch S, Pankratz M, Tatar M. Drosophila lifespan control by dietary restriction independent of insulin-like signaling. Aging Cell. 2008;7:199–206.

42. Paaby AB, Blacket MJ, Hoffmann AA, Schmidt PS. Identification of a candidate adaptive polymorphism for Drosophila life history by parallel independent clines on two continents. Mol Ecol. 2010;19:760–74.

43. Paaby AB, Bergland AO, Behrman EL, Schmidt PS. A highly pleiotropic amino acid polymorphism in the Drosophila insulin receptor contributes to life-history adaptation. Evolution. 2014;68:3395–409.

44. Emlen DJ, Warren IA, Johns A, Dworkin I, Lavine LC. A mechanism of extreme growth and reliable signaling in sexually selected ornaments and weapons. Science. 2012;337:860–4.

45. Gotoh H, Miyakawa H, Ishikawa A, Ishikawa Y, Sugime Y, Emlen DJ, et al. Developmental link between sex and nutrition; doublesex regulates sex-specific mandible growth via juvenile hormone signaling in stag beetles. PLoS Genet. 2014;10:e1004098.

46. Gotoh H, Cornette R, Koshikawa S, Okada Y, Lavine LC, Emlen DJ, et al. Juvenile hormone regulates extreme mandible growth in male stag beetles. PLoS One. 2011;6:e21139.

47. Zera AJ, Harshman LG. Laboratory selection studies of life-history physiology in insects. In: Experimental Evolution: Concepts, Methods, and Applications of Selection Experiments. University of California Press; 2009. p. 236–81.

48. King EG, Roff DA, Fairbairn DJ. The evolutionary genetics of acquisition and allocation in the wing dimorphic cricket, Gryllus firmus. Evolution. 2011;65:2273–85.

49. King EG, Roff DA, Fairbairn DJ. Trade-off acquisition and allocation in Gryllus firmus: a test of the Y model. J Evol Biol. 2011;24:256–64.

50. Flatt T, Tu M-P, Tatar M. Hormonal pleiotropy and the juvenile hormone regulation of Drosophila development and life history. Bioessays. 2005;27:999–1010.

51. Tatar M, Bartke A, Antebi A. The endocrine regulation of aging by insulin-like signals. Science. 2003;299:1346–51.

52. Zera AJ, Harshman LG, Williams TD. Evolutionary endocrinology: the developing synthesis between endocrinology and evolutionary genetics. Annu Rev Ecol Evol Syst. 2007;38:793–817.

53. Hughes KA, Reynolds RM. Evolutionary and mechanistic theories of aging. Annu Rev Entomol. 2005;50:421–45.

54. Remolina SC, Chang PL, Leips J, Nuzhdin SV, Hughes KA. Genomic basis of aging and life-history evolution in Drosophila melanogaster. Evolution. 2012;66:3390–403.

55. Burke MK, King EG, Shahrestani P, Rose MR, Long AD. Genome-wide association

study of extreme longevity in Drosophila melanogaster. Genome Biol Evol. 2014;6:1–11.

56. Magwire MM, Yamamoto A, Carbone MA, Roshina NV, Symonenko AV, Pasyukova EG, et al. Quantitative and molecular genetic analyses of mutations increasing Drosophila life span. PLoS Genet. 2010;6:e1001037.

57. Rockman MV. The QTN program and the alleles that matter for evolution: all that's gold does not glitter. Evolution. 2012;66:1–17.

58. Briga M, Verhulst S. What can long-lived mutants tell us about mechanisms causing aging and lifespan variation in natural environments? Exp Gerontol. 2015;71:21–6.

59. Savory FR, Benton TG, Varma V, Hope IA, Sait SM. Stressful environments can indirectly select for increased longevity. Ecol Evol. 2014-4;4:1176–85.

60. Pertea M, Kim D, Pertea GM, Leek JT, Salzberg SL. Transcript-level expression analysis of RNA-seq experiments with HISAT, StringTie and Ballgown. Nat Protoc. 2016;11:1650–67.

61. Stanley PD, Ng'oma E, O'Day S, King EG. Genetic dissection of nutrition-induced plasticity in insulin/insulin-like growth factor signaling and median life span in a *Drosophila* multiparent population. Genetics. 2017;206:587–602.

62. Stobdan T, Sahoo D, Azad P, Hartley I, Heinrichsen E, Zhou D, et al. High fat diet induces sex-specific differential gene expression in Drosophila melanogaster. PLoS One. 2019;14:e0213474.

63. Rivera O, McHan L, Konadu B, Patel S, Sint Jago S, Talbert ME. A high-fat diet impacts memory and gene expression of the head in mated female Drosophila melanogaster. J Comp Physiol B. 2019;189:179–98.

64. Heinrichsen ET, Zhang H, Robinson JE, Ngo J, Diop S, Bodmer R, et al. Metabolic and transcriptional response to a high-fat diet in Drosophila melanogaster. Molecular Metabolism. 2014;3:42–54.

65. Reed LK, Lee K, Zhang Z, Rashid L, Poe A, Hsieh B, et al. Systems genomics of metabolic phenotypes in wild-type Drosophila melanogaster. Genetics. 2014;197:781–93.

66. Musselman LP, Fink JL, Baranski TJ. Similar effects of high-fructose and high-glucose feeding in a Drosophila model of obesity and diabetes. PLoS One. 2019;14:e0217096.

67. Ng'oma E, Fidelis W, Middleton KM, King EG. The evolutionary potential of diet-dependent effects on lifespan and fecundity in a multi-parental population of Drosophila melanogaster. Heredity. 2018;:1.

68. Lee KP, Simpson SJ, Clissold FJ, Brooks R, Ballard JWO, Taylor PW, et al. Lifespan and reproduction in Drosophila: new insights from nutritional geometry. Proc Natl Acad Sci U S A. 2008;105:2498–503.

69. Jensen K, McClure C, Priest NK, Hunt J. Sex-specific effects of protein and carbohydrate intake on reproduction but not lifespan in Drosophila melanogaster. Aging Cell. 2015-8;14:605–15.

70. Dobson AJ, Ezcurra M, Flanagan CE, Summerfield AC, Piper MDW, Gems D, et al. Nutritional Programming of Lifespan by FOXO Inhibition on Sugar-Rich Diets. Cell Rep. 01 10, 2017;18:299–306.

71. Lakowski B, Hekimi S. The genetics of caloric restriction in Caenorhabditis elegans. Proc Natl Acad Sci U S A. 1998;95:13091–6.

72. Houthoofd K, Braeckman BP, Johnson TE, Vanfleteren JR. Life extension via dietary restriction is independent of the Ins/IGF-1 signalling pathway in Caenorhabditis elegans. Exp Gerontol. 2003;38:947–54.

73. Kaeberlein TL, Smith ED, Tsuchiya M, Welton KL, Thomas JH, Fields S, et al. Lifespan extension in Caenorhabditis elegans by complete removal of food. Aging Cell. 2006;5:487–94.

74. Lee GD, Wilson MA, Zhu M, Wolkow CA, de Cabo R, Ingram DK, et al. Dietary deprivation extends lifespan in Caenorhabditis elegans. Aging Cell. 2006;5:515–24.

75. Giannakou ME, Goss M, Partridge L. Role of dFOXO in lifespan extension by dietary restriction in Drosophila melanogaster: not required, but its activity modulates the response. Aging Cell. 2008;7:187–98.

76. Gershman B, Puig O, Hang L, Peitzsch RM, Tatar M, Garofalo RS. High-resolution dynamics of the transcriptional response to nutrition inDrosophila: a key role for dFOXO. Physiological Genomics. 2007;29:24–34. doi:10.1152/physiolgenomics.00061.2006.

77. Greer EL, Dowlatshahi D, Banko MR, Villen J, Hoang K, Blanchard D, et al. An AMPK-FOXO pathway mediates longevity induced by a novel method of dietary restriction in C. elegans. Curr Biol. 2007;17:1646–56.

78. Narasimhan SD, Yen K, Tissenbaum HA. Converging pathways in lifespan regulation. Curr Biol. 2009;19:R657–66.

79. Santos J, Leitão-Correia F, Sousa MJ, Leão C. Dietary Restriction and Nutrient Balance in Aging. Oxid Med Cell Longev. 2016;2016:4010357.

80. Partridge L, Piper MDW, Mair W. Dietary restriction in Drosophila. Mech Ageing Dev. 2005;126:938–50.

81. Poulose SM, Miller MG, Scott T, Shukitt-Hale B. Nutritional Factors Affecting Adult

Neurogenesis and Cognitive Function. Adv Nutr. 2017;8:804–11.

82. Arslan-Ergul A, Ozdemir AT, Adams MM. Aging, neurogenesis, and caloric restriction in different model organisms. Aging Dis. 2013;4:221–32.

83. Martínez G, Duran-Aniotz C, Cabral-Miranda F, Vivar JP, Hetz C. Endoplasmic reticulum proteostasis impairment in aging. Aging Cell. 2017;16:615–23.

84. Newberg LA, Chen X, Kodira CD, Zavodszky MI. Computational de novo discovery of distinguishing genes for biological processes and cell types in complex tissues. PLoS One. 2018;13:e0193067.

85. King EG, Merkes CM, McNeil CL, Hoofer SR, Sen S, Broman KW, et al. Genetic dissection of a model complex trait using the Drosophila Synthetic Population Resource. Genome Res. 2012;22:1558–66.

86. King EG, Macdonald SJ, Long AD. Properties and power of the Drosophila Synthetic Population Resource for the routine dissection of complex traits. Genetics. 2012;191:935–49.

87. Ng'oma E, King EG, Middleton KM. A model-based high throughput method for fecundity estimation in fruit fly studies. Fly . 2018. doi:10.1080/19336934.2018.1562267.

88. Bass TM, Grandison RC, Wong R, Martinez P, Partridge L, Piper MDW. Optimization of dietary restriction protocols in Drosophila. J Gerontol A-Biol. 2007;62:1071–81.

89. Kim D, Langmead B, Salzberg SL. HISAT: a fast spliced aligner with low memory requirements. Nat Methods. 2015;12:357–60.

90. Li H, Handsaker B, Wysoker A, Fennell T, Ruan J, Homer N, et al. The Sequence Alignment/Map format and SAMtools. Bioinformatics. 2009;25:2078–9.

91. Pertea M, Pertea GM, Antonescu CM, Chang T-C, Mendell JT, Salzberg SL. StringTie enables improved reconstruction of a transcriptome from RNA-seq reads. Nat Biotechnol. 2015;33:290–5.

92. Love MI, Huber W, Anders S. Moderated estimation of fold change and dispersion for RNA-seq data with DESeq2. Genome Biol. 2014;15:550.

93. Leek JT, Storey JD. Capturing heterogeneity in gene expression studies by surrogate variable analysis. PLoS Genet. 2007;3:e161.

94. Leek JT. svaseq: removing batch effects and other unwanted noise from sequencing data. Nucleic Acids Res. 2014;42. doi:10.1093/nar/gku864.

95. Luo W, Friedman MS, Shedden K, Hankenson KD, Woolf PJ. GAGE: generally applicable gene set enrichment for pathway analysis. BMC Bioinformatics. 2009;10:161.

96. Kanehisa M, Goto S. KEGG: kyoto encyclopedia of genes and genomes. Nucleic Acids Res. 2000;28:27–30.

97. Benjamini Y, Hochberg Y. Controlling the false discovery rate: a practical and powerful approach to multiple testing. J R Stat Soc Series B Stat Methodol. 1995;57:289–300.

98. Langfelder P, Horvath S. WGCNA: an R package for weighted correlation network analysis. BMC Bioinformatics. 2008;9:559.

99. Langfelder P, Horvath S. FastRFunctions for Robust Correlations and Hierarchical Clustering. Journal of Statistical Software. 2012;46. doi:10.18637/jss.v046.i11.

100. Dong J, Horvath S. Understanding network concepts in modules. BMC Syst Biol. 2007;1:24.

101. Sikkink KL, Reynolds RM, Ituarte CM, Cresko WA, Phillips PC. Environmental and evolutionary drivers of the modular gene regulatory network underlying phenotypic plasticity for stress resistance in the Nematode Caenorhabditis remanei. G3. 2019;9:969–82.

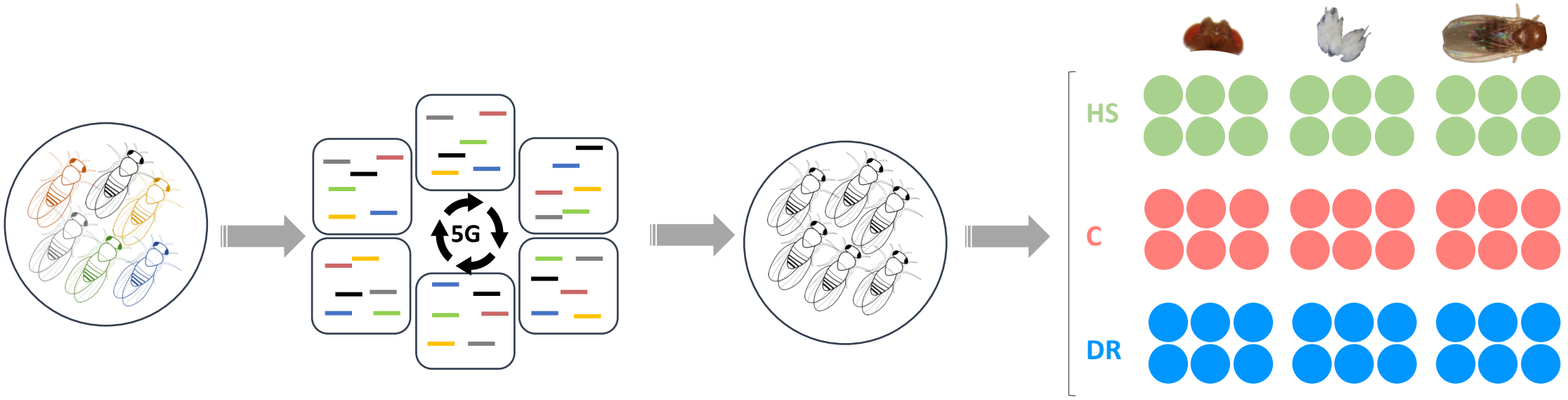
5G
HS
C
DR
835 RILs
Generate a homogenous base population
An outbred base population
Day 12-22 post-oviposition: treatment diet

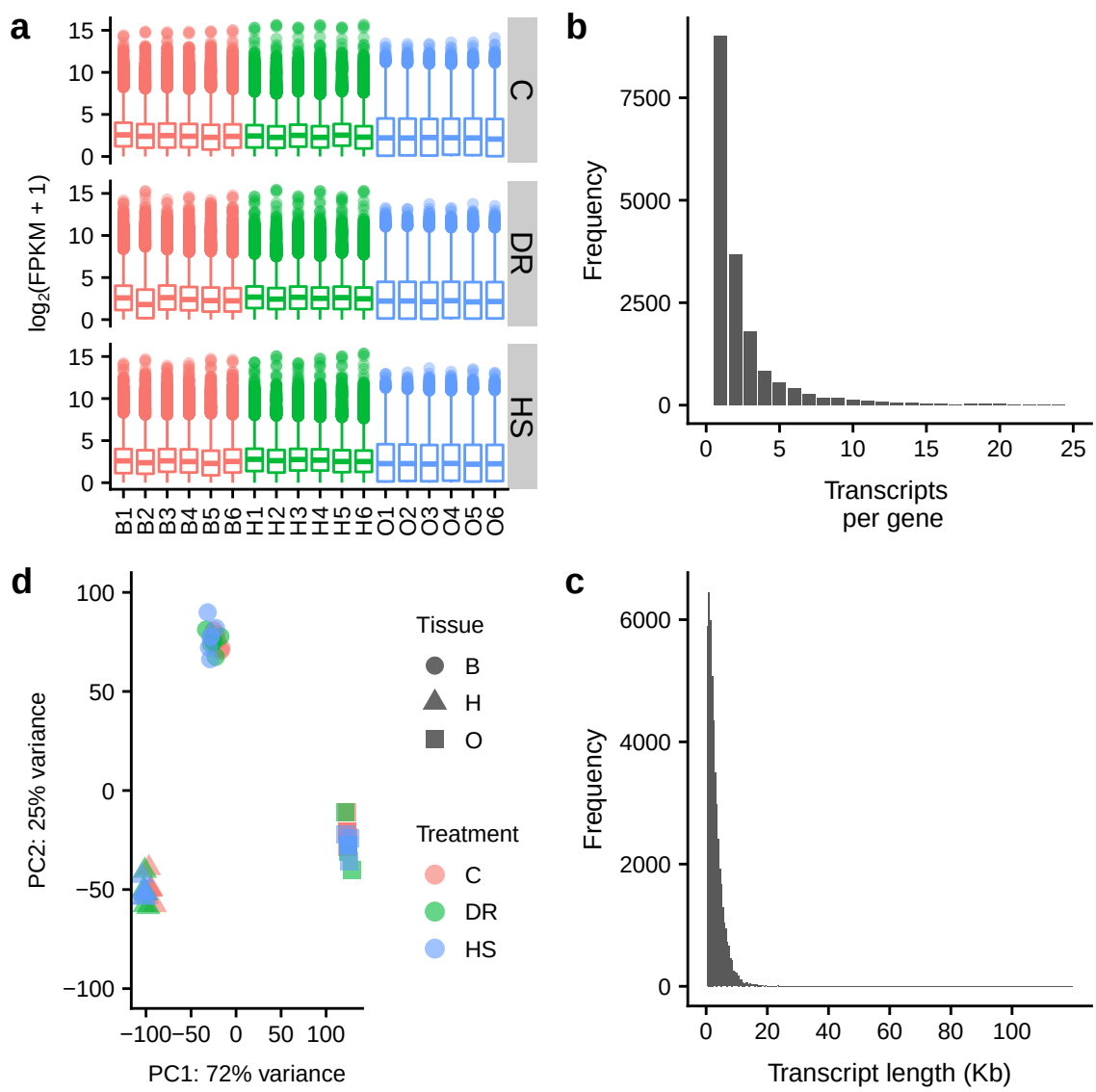
a
log2(FPKM + 1)
C
DR
HS
B1
B2
B3
B4
B5
B6
H1
H2
H3
H4
H5
H6
O1
O2
O3
O4
O5
O6
b
Frequency
Transcripts per gene
c
Frequency
Transcript length (Kb)
d
PC2: 25% variance
PC1: 72% variance
Tissue
B
H
O
Treatment
C
DR
HS

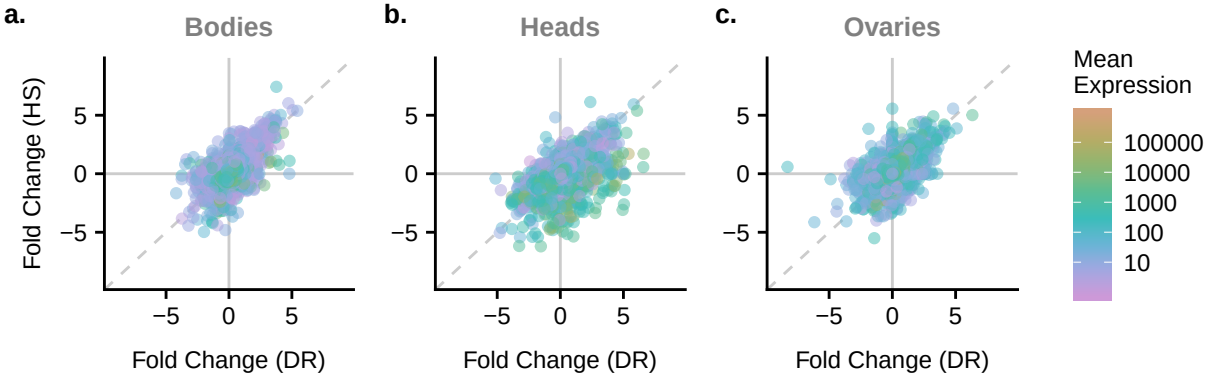
a.
Bodies
b.
Heads
c.
Ovaries
Fold Change (HS)
5
0
−5
−5
0
5
Fold Change (DR)
Mean
Expression
100000
10000
1000
100
10

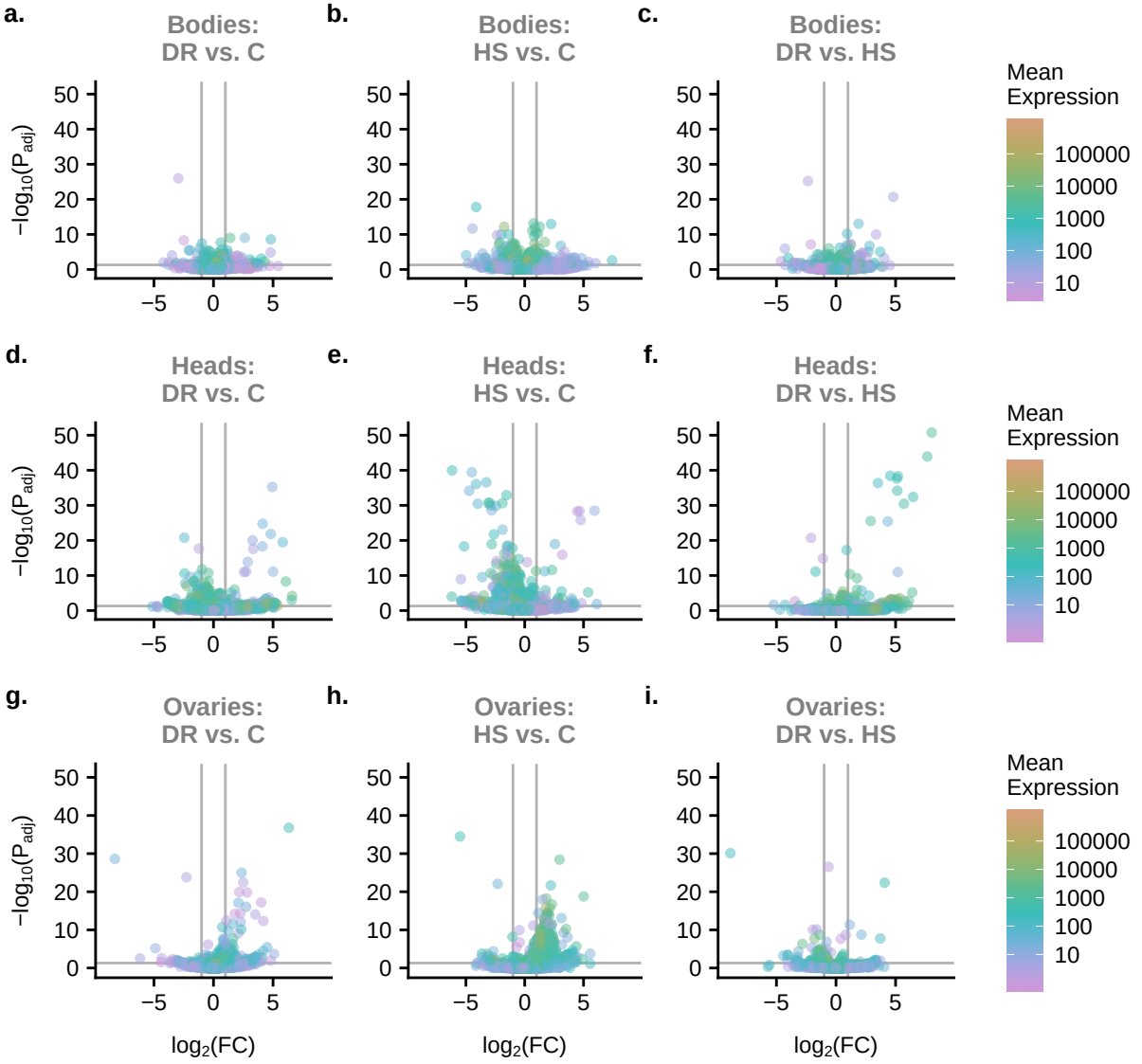
a.
Bodies:
DR vs. C
b.
Bodies:
HS vs. C
c.
Bodies:
DR vs. HS
d.
Heads:
DR vs. C
e.
Heads:
HS vs. C
f.
Heads:
DR vs. HS
g.
Ovaries:
DR vs. C
h.
Ovaries:
HS vs. C
i.
Ovaries:
DR vs. HS
−log10(Padj)
log2(FC)
Mean
Expression
100000
10000
1000
100
10

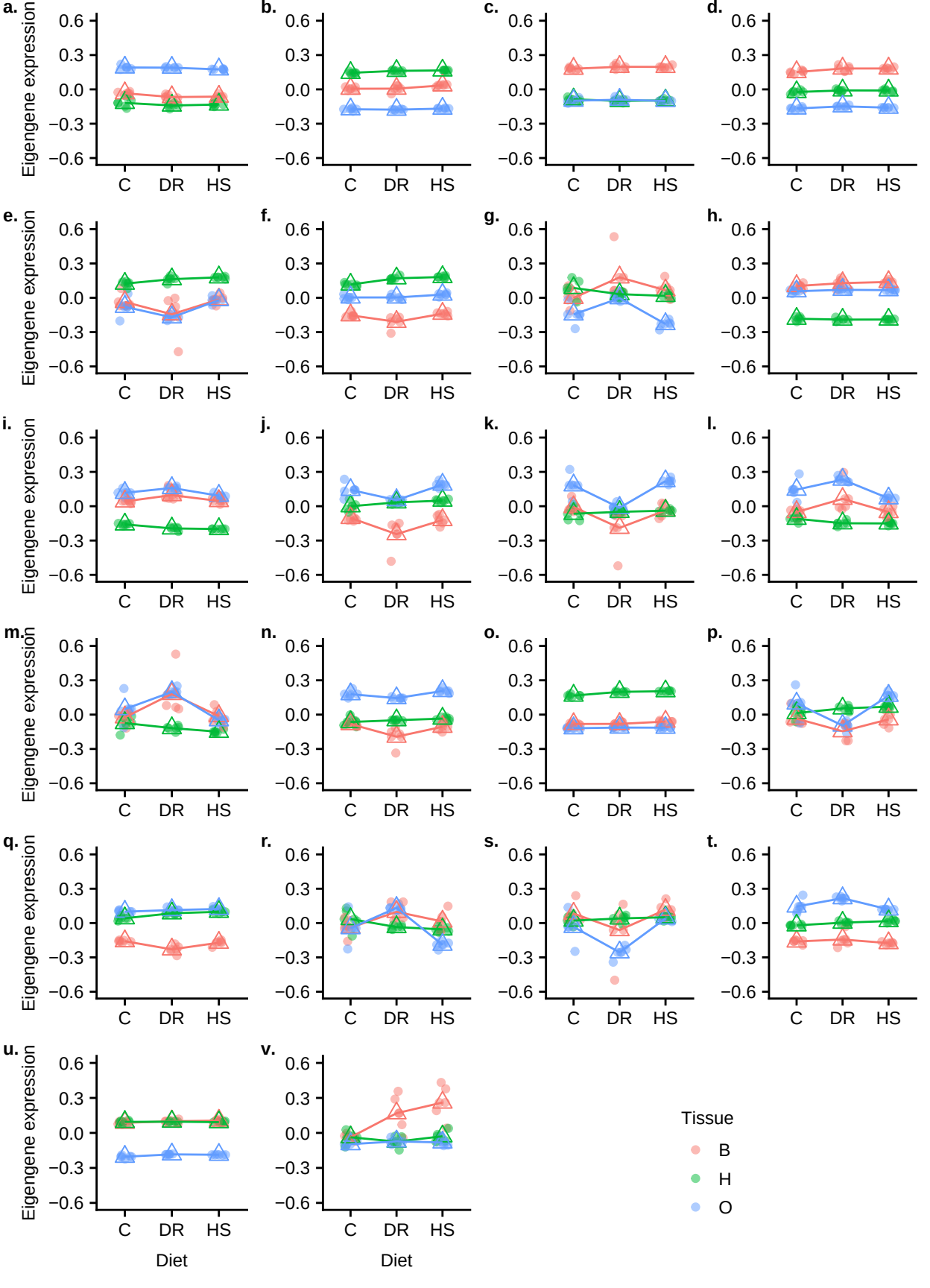
a.
b.
c.
d.
e.
f.
g.
h.
i.
j.
k.
l.
m.
n.
o.
p.
q.
r.
s.
t.
u.
v.
Eigengene expression
0.6
0.3
0.0
−0.3
−0.6
C
DR
HS
Diet
Tissue
B
H
O